

THE COMPARISON OF THE BAYER PROCESS WASTES ON THE BASE OF CHEMICAL AND PHYSICAL PROPERTIES

A. Atasoy*

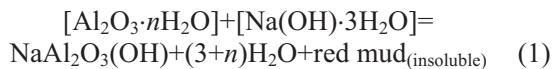
University of Sakarya, TEF, Extractive Metallurgy Division, Esentepe, 54187 Adapazari, Turkey

In this work, the waste materials from the Aughinish (in Ireland) and the Seydisehir (formerly ETI Aluminium Inc. in Turkey) alumina plants were compared on the base of chemical and the physical properties using thermal analysis, XRD and SEM techniques. The results were shown that there are big differences in the chemical compositions of the red mud waste as well as the physical properties. It was found that the Seydisehir red mud is more feasible for recovery of iron, but the Aughinish sample contains more titanium oxide than the Seydisehir one. There are also some variations in the Bayer process of the plants since the calcium and sodium oxides of the waste were different percentages.

Keywords: Aughinish red mud, bauxite waste, comparison, Seydisehir red mud

Introduction

Bauxite is main ore for production of alumina by using the Bayer process [1]. The colour of the ore shows the iron content of it. Generally, it finds in tropical countries [2–4]. It consists of hydrated oxides of alumina mixed with iron oxide, silica, calcium oxide and other minor constituents which are separated as an insoluble waste after the recovering of hydrated alumina from the Bayer process [2–5].



The reaction given above can be explained of the formation of soluble sodium aluminum hydroxide and the generation of the insoluble solid residue in the process. During the production of one tone of alumina, 1.5 t. of solid waste generates which is called red mud. Consequently, there are millions tones of red mud storaged beside of plants, in disposal areas [4], which create lot of problems [4–6]. On the other hand, red mud contains considerable amount of un-recovered alumina, iron oxide and titan. In some of red muds, there are considerable amount of rare earth elements, such as Zr, U, Nb, V and Th [7, 8]. It has been reported that the percentages of rare elements in the red mud are higher when compared with their average distribution in the earth crust [6]. There are many attempts concerning extraction of valuable oxides or utilisation of red muds have been put forward in building materials [9–12], metallurgical [13–16], or chemical [17] and other applications [18, 19].

The mineralogical composition of red mud depends on bauxite and the Bayer process. There are several investigations on the mineralogical composition of the red muds [20, 21]. Hematite is main and dominant phase in the presence of alumina phases either gibbsite ($\text{Al}(\text{OH})_3$) or boehmite, $\text{AlO}(\text{OH})$.

It is possible to characterize red mud by thermal, chemical, physical and morphological properties using various characterisation methods. Some fundamental studies concerning the characterisation of red mud by the TG/DTA analysis are available [22, 23]. Generally, three endothermic peaks were determined on DTA curve at temperatures between 280–350°C, in presence of goethite phase. The first peak was attributed to goethite phase and the second and the third peaks were attributed to the loss of water from gibbsite and goethite. It was reported that the Aughinish red mud sample has three endothermic peaks within the 250–350°C temperature ranges [21]. Those peaks indicate loss of water from goethite and gibbsite.

In the present work, the comparison of the alumina wastes from different plants was made based on the characterisations, thermal analysis, particle size and morphology of the red mud samples. The work was carried out by using X-ray diffraction, scanning electron microscope, simultaneous thermal analysis methods.

Experimental

In this work, two different Bayer waste materials, from the Aughinish alumina plant (Shannon, Limerick-Ire-

* aatasoy@sakarya.edu.tr

land) [24] and the Seydisehir alumina plant (Seydisehir, Konya-Turkey) were studied. The both samples were mixture of solid and water in different percentages.

Thermal analysis of the Aughinish red mud was carried out on a Seiko SSC/5200 thermal analysis system. X-ray diffraction analysis was performed on a Philips 3020 diffractometer CuK α equipped with a graphite monochromator. Philips 525 scanning electron microscope (SEM) was used for particle and surface morphology of the Aughinish red mud sample. The experiments on the Aughinish red mud sample were carried out in the laboratories in the Manchester Materials Science Centre-UMIST.

The chemical analysis and surface morphology of the Seydisehir red mud sample was performed on a JOEL JSM-6060LV (SEM) scanning electron microscope equipped with an energy dispersive analytical X-ray (EDAX) system. Simultaneous thermal analysis TG/DTA measurement was provided from elsewhere [25] in the range 20–1200°C in air atmosphere condition. X-ray diffraction analysis of the Seydisehir red mud sample was carried out on a Rigaku-DMAX 2200 diffractometer. The crystalline phases in the red mud samples were identified using the data to powder diffraction files complied by JCPDS. The experiments on the Seydisehir red mud sample were carried at the University of Sakarya.

The more details, regarding the physical, chemical and mineralogical properties of the Seydisehir red mud were presented and compared with the previous study on the Aughinish red mud sample [20] in the following part of the work.

Results and discussion

There are some differences in production capacities and bauxite source between two plants. The annual alumina production capacity of the Aughinish alumina plant is around 1000000 t. While, the Seydisehir capacity is 200000 t which equals to 1/5 of the Aughinish plant. The Aughinish alumina plant imports its bauxite requirement from Guinea in West Africa [24], but the bauxite requirement in the Seydisehir alumina plant extracts it from local sources.

The chemical composition of the bauxites is presented in Table 1. As seen from the table, the aluminium oxide content of the ores are almost the same, but some differences with the minor

Table 1 The chemical composition of the bauxite ores used

Oxides	Aughinish [24]	Seydisehir [26]
Al ₂ O ₃	56.2±3.9	57.00
Fe ₂ O ₃	10.2±4.13	17.5
TiO ₂	4.0±1.2	2.5
SiO ₂	1.4±1.6	8.00
CaO	0.07±1.2	0.75
Na ₂ O	—	—
other	—	—
total	78.6±13.4	87.75
L.O.I.	7.9	12.5

constituents or the insoluble residue content has been seen. Especially, the silica content in the Seydisehir bauxite is 5 times higher than the Aughinish Alumina Plant ones. The iron ratio in the Seydisehir bauxite is also higher than the bauxite used in the Aughinish plant. Calcium oxide percentage is quite low in both bauxite ores. It is added during the process to remove unwanted carbonates and phosphates. As expected the variations in the bauxite compositions in turn alters the condition of the Bayer process and parameters such as temperature and pressure, amount of caustic soda addition.

After the recovery of aluminium oxide content of the bauxites, the percentages of the unwanted oxides are increased to the levels presented in Table 2. As expected Fe₂O₃, Al₂O₃, SiO₂, TiO₂, CaO and Na₂O present in the both of the samples with various percentages. The un-recovered aluminium oxide was one of the major oxide in the both red mud samples, but alumina content is lower in the Seydisehir red mud sample (20.24%) than the Aughinish one (23.6%). There are large differences in the titanium content of the red mud samples which is very important for the utilisation of red mud for extraction of pigment from it. The Aughinish red mud sample has high titan content (17.85%) compared with the analysis of the Seydisehir red mud (4.15%). It comes from bauxite ore. It is possible to suggest that the use of the Seydisehir red mud for production of iron is more feasible than the Aughinish red mud.

Silica and calcium oxide content are also important to show the Bayer process variations in the plants. Calcium oxide is added during the Bayer process to facilitate unwanted carbonates. As seen from Table 1, there is no sodium oxide content in the bauxites although it has been detected in the red mud wastes Table 2. Sodium oxide is added to recovery of

Table 2 The basic composition of the red muds generated in the plants

Sample/oxide%	Al ₂ O ₃	Fe ₂ O ₃	TiO ₂	SiO ₂	CaO	Na ₂ O	other	total
Aughinish	23.6	30.4	17.85	9.65	6.4	5.3	6.8	100
Seydisehir	20.24	39.84	4.15	15.24	1.80	9.43	0.48	100

aluminium content of the bauxite ore. The Seydisehir red mud sample has higher sodium hydroxide content than the Aughinish sample. There are proportional relationships between sodium content of the waste with the un-recovered aluminium hydroxide content. It is clear that there is some portion of unrecovered sodium aluminates content in the both red mud samples. The differences in the sodium content of the sample may come from the variations of the washing units. The improvements in the washing operation or rewashing and filtering, can used for recovery of valuable sodium aluminates content of the red mud.

Iron oxide, alumina and titan can be defined as valuable oxide in the red muds. The total percentage of these valuable oxides is approximately 75% in the Aughinish sample and nearly 65% in the Seydisehir sample. The red mud waste from the both plants is a potential resource for production of one or more oxides. The utilisation of the Aughinish red mud can be used for extraction of iron oxide or ferrotitanium. After the removing of iron content of the red mud, the remained solid residue can be used as a raw material in ceramic production. However, the Seydisehir red mud seen more beneficial for the production of iron. It is seen that the Seydisehir red mud is more useful in metallurgical applications than the Aughinish sample.

The mineralogical compositions of the samples were determined using X-ray diffraction analysis (Figs 1 and 2). The identified mineral phases in the Seydisehir red mud are Hematite (Fe_2O_3 card no. 33-0664), Gibbsite ($\text{Al}(\text{OH})_3$ card no. 33-180), Sodalite ($\text{Na}_8\text{Al}_6\text{Si}_6\text{O}_{24}$ card no. 16-0612), Calcium Silicates (CaSiO_3 card no.), Boehmite ($\text{AlO}(\text{OH})$ card no. 21-1307), Goethite ($\text{FeO}(\text{OH})$ card no. 26-0792), Sodalite ($\text{Na}_2\text{O}\cdot\text{Al}_2\text{O}_3\cdot\text{SiO}_2$, card no. 16-0612), Calcium Aluminum Silicate ($\text{Ca}_2\text{Al}_2(\text{SiO}_4)(\text{OH})_8$ card no. 03-0798). The Aughinish red mud contains more mineral phases than the Seydisehir red mud. Addition of these, rutile (TiO_2 card no. 21-1276), perowskite (CaTiO_4 , card no. 22-0153) and quartz (SiO_2 , card no. 18-1166) are present in the Aughinish sample. Since calcium oxide content of the Aughinish red mud is high, it reacts with titanium oxide for the formation of calcium titanate. The mineralogical compositions of the red muds can be changed by the type of bauxite used in the plants and the Bayer process parameters.

A comparison of Figs 1 and 2 indicate that there were large pattern differences between red mud samples. It is clear that, the formation of new phases is dominant in the Aughinish red mud sample. But the old phases are major peaks in the SRM sample. As predicted hematite was one of the major phase in the both samples, but it was dominant in the Seydisehir ones. Boehmite and gibbsite are also determined in

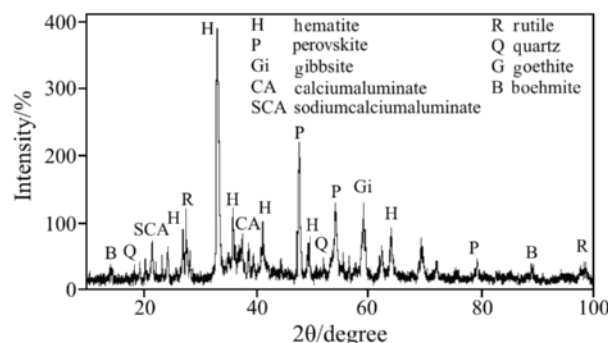


Fig. 1 X-ray diffraction patterns of the Seydisehir sample

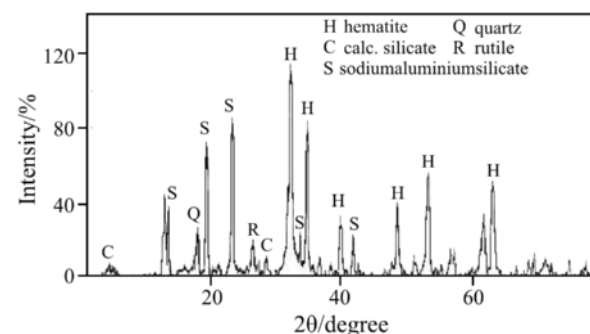


Fig. 2 X-ray diffraction pattern of the Seydisehir red mud

the red mud. These mineral phases come from the bauxite used in the plants. The determined old mineral phases were directly transferred to the red mud from the bauxite ores without any change. According to the XRD pattern of the samples, CaO , Na_2O and SiO_2 were found in the form of calcium silicate, sodium titan and sodium silicate, as a result of the costic soda leaching.

To be understood the thermal behavior of the samples and any reactions were carried out during the heating thermogravimetric analysis (TG) and differential thermal analysis (DTA) is most powerful and common method. The simultaneous TG/DTA curves for each red mud sample are presented in Figs 3 and 4. It is possible to compare the DTA curves of the red mud samples on the number of endothermic peaks and temperatures. Since the chemical compositions of the samples vary, the TG/DTA curves of them will be different form. As seen from the curves, there are some variations in the size of the endothermic peaks as well as temperatures. There are series of endothermic peaks within 250–300°C ranges, a small peak at temperature 500°C, another visible peak at around 1150–1200°C in the Aughinish red mud sample. They may be small peak as inflection of variable size on the peaks. The endothermic peak at 250–300°C can be related with the decomposition of gibbsite to form $\alpha\text{-Al}_2\text{O}_3$. There are series of

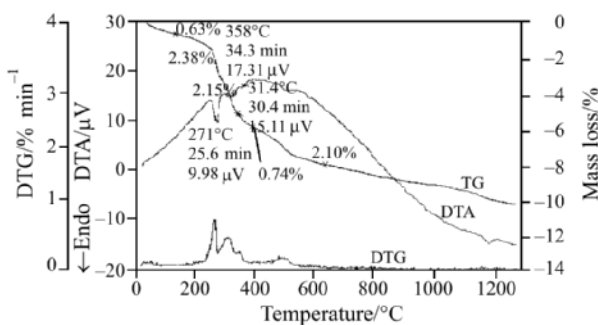


Fig. 3 TG/DTG and DTA curves of the Aughinish red mud [20]

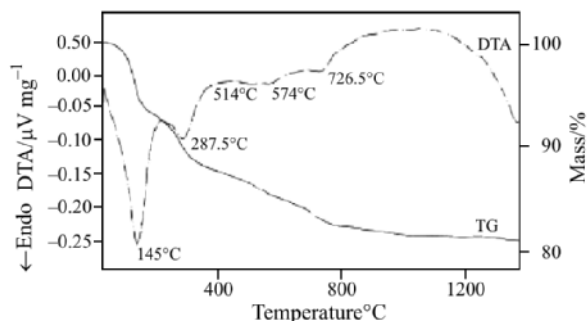
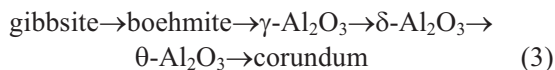


Fig. 4 DTA/TG analysis of the Seydisehir red mud sample [25]

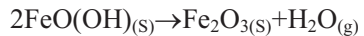
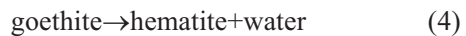
transformation in alumina until corundum structure which covers temperature between 250–900°C.



As seen above equations, gibbsite partially dehydroxylates to boehmite at temperature 270°C and the remained part of the gibbsite goes to a transition of alumina at 314°C. There are different suggestions on the DTA curve of the gibbsite [22–24].

The differential thermal analysis curve of the Seydisehir red mud is given in Fig. 4. There are visible differences on the DTA curves of the samples.

The endothermic peaks occur at temperatures 145, 287, 514, 574 and 726°C. The first peak at 145°C is related with the evaporation of physical water content of the red mud. The second peak at 287°C corresponds gibbsite decomposition to boehmite. The peak around 730°C could be related with the decomposition of calcite phase in the sample. Any observed endothermic peaks above 800°C could be explained by decomposition of sodalite phases in the red mud sample. Quartz shows also transition at around 550°C. Above 1000°C, there may be formed new phases, such as Fe_2TiO_4 , as a result of the reactions between iron oxide and titanium oxide. The small endothermic peaks can be explained with the loose of water form or any volatile content of the mineral phases such as CaCO_3 . The dehydration of goethite FeO(OH) in the red mud takes place according to the following reaction.



Thermogravimetric curves of the samples are given in Figs 3 and 4. It can be seen that there is very fast mass loss up to 150°C which corresponds 8%. At this temperature the mass loss of the sample can be explained with the loss of physical water content of the sample. At temperature within 150–300°C the mass loss of the sample is around 5% which is associated with the loss of water from the gibbsite and goethite phases. The total mass loss of the Seydisehir red mud sample is around 19% is higher than the Aughinish red mud with the value of 10%. The summary of the thermogravimetric and differential thermal analysis of the red mud samples was presented in Table 3.

The SEM micrograph of the samples were presented in Figs 5 and 6. As seen from the pictures that the both samples are composed of very fine particles. The particles have rounded and flakes shapes. The particle size range a few micron to 10 microns. The Seydisehir red mud has coarse particle as the

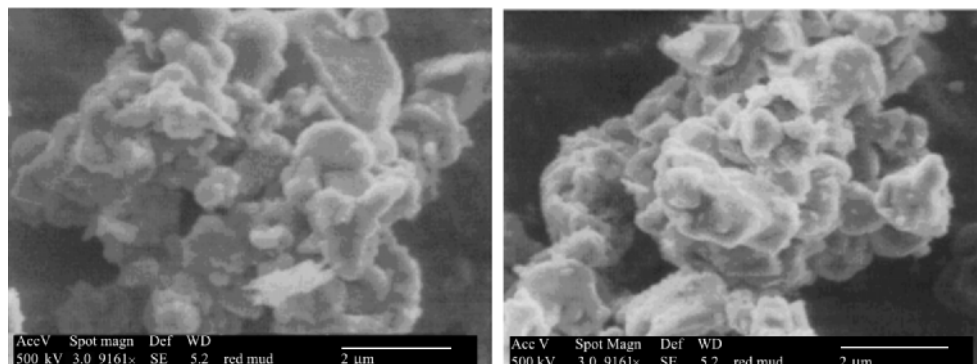
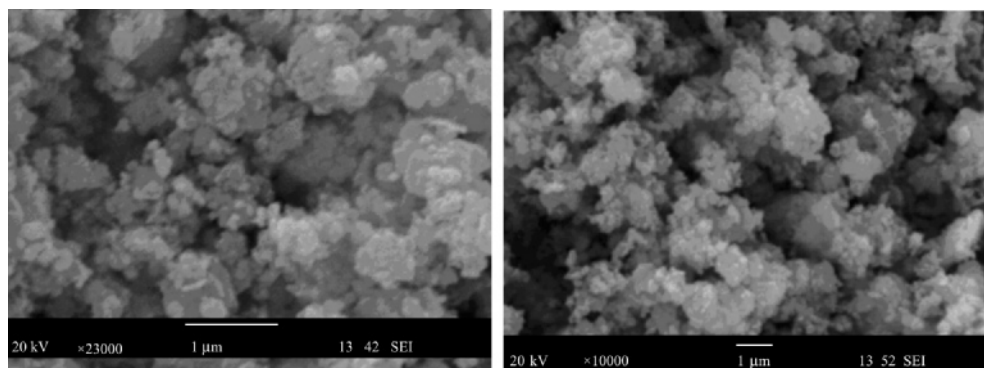


Fig. 5 SEM pictures of the Aughinish red mud sample

**Fig. 6** SEM pictures of the Seydisehir red mud sample**Table 3** Summary of the thermal analysis of the samples

Peaks and mass loss	Temperature/°C	Explanations
Endothermic (Aughinish)		
1. peak	271	
2. peak	314	
3. peak	358	Dehydration of
4. peak	560	Formation of boehmite and γ -alumina
5. peak	570	Decomposition of goethite to hematite
6. peak	900	
7. peak	1150	
Endothermic (Seydisehir)		
1. peak	145	Evaporation of the physical water
2. peak	280	Gibbsite decomposition
3. peak	514	Boehmite decomposition
4. peak	574	Diaspora formation
5. peak	726	Calcite decomposition
Mass loss – Aughinish		
1. region	0–230	1.3%
2. region	230–280	1.7%
3. region	280–360	2.5%
4. region	360–480	1.3%
5. region	480–550	0.8%
6. region	550–1150	2.1%
7. region	1150–1200	0.2%
8. region	$T < 1200$	0.3%
total		10.2%
Mass loss – Seydisehir		
1. region	0–150	5%
2. region	150–260	4%
3. region	260–300	2%
4. region	300–530	2%
5. region	530–580	1%
6. region	580–700	1.5%
7. region	700–780	1.5%
8. region	780–980	1%
9. region	980–1200	1%
total		19%

Aughinish sample. The coarse particle would represent iron and other unchanged minerals during the Bayer process. The density of Seydisehir red mud was found to be 3.05 g cm^{-3} which is denser than the Aughinish red mud sample (2.85 g cm^{-3}). It is possible to suggest that, the differences in density of the sample come from the differences in the chemical compositions of the samples.

Conclusions

The chemical, mineralogical and thermal evaluations of two different red mud samples were made in this work by different characterisation methods. There are big differences in the origin and the chemical composition bauxites used in the plants. The ores are determined the Bayer process parameters and caustic

soda addition. There are huge gap in the annual capacity of alumina production of the plants which result generation of large amount of red mud waste. There are slight changes in the aluminum hydroxide content of the ores, but the titanium oxide content of the ores is different.

The wastes from the plants contain considerable amount of valuable oxides which are un-recovered alumina, iron and titanium oxides. Iron oxide is dominant phase in the both samples but the Seydisehir red mud sample can be more feasible in the metallurgical application. On the other hand, the recovery of titan is more economical in the Aughinish red mud. The variations in Na₂O and CaO content of the samples indicate that there are differences in the operation parameters of the plants since they are added to recovery of aluminum content in the bauxite ore and to increase the efficiency of the Bayer process.

References

- 1 K. J. Bayer, German Patent No: 2150677, 1972.
- 2 B. K. Parekh, Proc. 6th Min. Waste Utilization Symp., 6 (1976) 123.
- 3 B. K. Parekh and W. Goldberger, Report no: EPA-600/2-76-301, 1976.
- 4 R. S. Thakur and S. N. Das, Red mud analysis and utilisation, PID and Wiley Eastern, New Delhi 1994.
- 5 L. Merkin, Ph.D. Thesis, Manchester University, 1996.
- 6 A. Atasoy, MSc Dissertation, UMIST 1996.
- 7 V. G. Logomerac, Travaux Con. Proc., 15 (1979) 279.
- 8 L. V. Tsakanika, M. T. Ochsenkuln-Petropoulou and L. N. Mendrinos, J. Anal. Bioanal. Chem., 379 (2004) 786.
- 9 N. Yalcin and V. Sevinc, Ceram. Int., 26 (2000) 485.
- 10 J. C. Knight, A. S. Wagh and W. A. Reid, J. Mater. Sci., 21 (1986) 2179.
- 11 W. R. Pinnock and J. N. Gordon, J. Mater. Sci., 27 (1992) 692.
- 12 Y. Lui, Patent no: CN 110053, 1998.
- 13 O. G. Frusman, USBM Investigation no: 7454, 1970.
- 14 F. P. Piga and L. Staoppa, JOM 45, 11 (1993) 55.
- 15 P. M. Parasad, J. S. Kachawha, R. C. Gupta, T. R. Mankhand and J. M. Sharma, Ligth metals science and technology, N. G. Anatraman, S. L. Malhatra, P. M. Parasad and C. Suryanarayana, Eds, Trans. Tech. Publication, Switzerland 1985, p. 31.
- 16 P. M. Parasad, Non-ferrous extractive metallurgy in the new millennium, NML, India 1999, p. 385.
- 17 E. Shannon and K. I. Vergese, J. Water Poll. Fed., 48 (1976) 1948.
- 18 A. S. Wagh and V. E. Douse, J. Mater. Res., 6 (1991) 1094.
- 19 V. M. Sgavlo, R. Compostrini, S. Maurina, G. Carturan, M. Monagheddu, G. Budroni and G. Cocco, J. Eur. Ceram. Soc., 20 (2000) 245.
- 20 A. Atasoy, J. Therm. Anal. Cal., 81 (2005) 357.
- 21 T. Tauber, R. K. Hill, D. N. Crook and M. J. Murray, J. Austr. Ceram. Soc., 7 (1971) 12.
- 22 R. Mackenzie, Differential Thermal Analysis, Vol. 1, Academic Press, London 1972.
- 23 W. Lodding, Thermal Analysis, Academic Press, London 1969.
- 24 Aughinish Alumina Magazine, 1984.
- 25 A. Alp and S. Goral, J. Therm. Anal. Cal., 73 (2003) 201.
- 26 www.mineral.org.tr

Received: April 25, 2006

Accepted: August 15, 2006

OnlineFirst: February 13, 2007

DOI: 10.1007/s10973-005-7671-y